Biosensors and Bioelectronics 190 (2021) 113372

Contents lists available at ScienceDirect

Biosensors and Bioelectronics

journal homepage: www.elsevier.com/locate/bios

Amplified and label-free electrochemical detection of a protease biomarker by integrating proteolysis-triggered transcription

Kai Shi, Lei Cao, Fang Liu, Shiyi Xie, Shuo Wang, Yan Huang, Chunyang Lei *, Zhou Nie

State Key Laboratory of Chemo/Biosensing and Chemometrics, College of Chemistry and Chemical Engineering, Hunan Provincial Key Laboratory of Biomacromolecular Chemical Biology, Hunan University, Changsha, 410082, PR China

ARTICLE INFO

Keywords:
Signal amplification
Synthetic biology
Electrochemical biosensor
MMP-2
RNA polymerase

ABSTRACT

Cell-free synthetic biology provides a promising strategy for developing high-performance biosensors by integrating with advanced testing technologies. However, the combination of synthetic biology with electrochemical testing techniques is still underdeveloped. Here, we proposed an electrochemical biosensor for the label-free and ultrasensitive detection of target protease biomarker by coupling a protease-responsive RNA polymerase (PR) for signal amplification. Taking tumor biomarker matrix metalloprotease-2 (MMP-2) as a model protease, we employed PR to transduce each proteolysis reaction mediated by MMP-2 into multiple programmable RNA outputs that can be captured by the DNA probes immobilized on a gold electrode. Moreover, the captured RNAs are designed to contain a guanine-rich sequence that can form G-quadruplex and bind to hemin in the presence of potassium ions. In this scenario, the activity of MMP-2 is converted and amplified into the electrochemical signals of hemin. Under the optimal conditions, this PR-based electrochemical biosensor enabled the sensitive detection of MMP-2 in a wide linear dynamic range from 10 fM to 1.0 nM, with a limit of detection of 7.1 fM. Moreover, the proposed biosensor was further applied in evaluating MMP-2 activities in different cell cultures and human tissue samples, demonstrating its potential in the analysis of protease biomarkers in complex clinical samples.

1. Introduction

With the standardization and modularization of artificial biological systems to create programmable functions, synthetic biology provides many specific target recognition elements for the construction biosensors (Ausländer et al., 2017; Courbet et al., 2015; Riglar et al., 2017; Mimee et al., 2018). Over the past decades, whole-cell synthetic biology has made significant progress in the field of biosensors (Watstein and Styczynski, 2018; Wan et al., 2019; Kotula et al., 2014; Saltepe et al., 2021). While the whole biosensors require a cellular host, which faces limitations in mass transfer disorders, cytotoxicity, genetic instability et al. (Keasling, 2012; Carlson et al., 2012; Silver et al., 2020). Cell-free synthetic biosensors have emerged as an alternative solution to address these challenges because of their simplicity, rapidity and high degree of freedom (Kopniczky et al., 2020; Jung et al., 2020). Most of the reported cell-free synthetic biosensors utilized fluorimetry and colorimetry as the signal detection modes, but they usually suffer from insufficient sensitivity or the requirement of sophisticated instruments (Wang et al., 2016; Hua et al., 2019). Recently, Kelley and Pardee et al. developed a multiplexed electrochemical sensor for the sensitive and specific detection of antibiotic resistance genes by operating cell-free gene circuits on electrochemical interfaces (Mousavi et al., 2020). In this work, they adopted a cell-free protein expression system to transduce target genes into different restriction enzyme outputs that generate different electrochemical signal patterns on microelectrode arrays. Liu et al. described an integrated biochemical circuit for high-resolution electrochemistry-based genetic analysis (Dai et al., 2020). This design converted the target gene locus into multiple programmable ssDNA outputs that can produce electrochemical signals by coupling the CRISPR-Cas9 system and primer exchange reaction. These studies provide feasible strategies for the rational combination of cell-free synthetic biology and electrochemical interface, exhibiting great potential in point-of-care diagnosis. Encouraged by these research progresses, we are interested in exploring a new paradigm for the construction of cell-free synthetic biology-based electrochemical biosensors.

Proteases regulate numerous critical physiological processes, including protein digestion (Bordusa, 2002), blood coagulation (Turk, 2006), cell growth, and differentiation (Bories et al., 1989). The

* Corresponding author.
E-mail address: cylei@hnu.edu.cn (C. Lei).

https://doi.org/10.1016/j.bios.2021.113372
Received 1 March 2021; Received in revised form 14 May 2021; Accepted 20 May 2021
Available online 5 June 2021

unregulated proteolysis can lead to many diseases, such as various cancers (Kang et al., 2008), immune diseases (Demeyer et al., 2016), Alzheimer's disease (Haass and Strooper, 1999), and inflammation (Lo et al., 2002). For example, matrix metalloproteinases (MMPs) are a class of secreted zinc-dependent endopeptidases involved in the degradation and processing of extracellular matrix and overexpress in almost all types of human tumors (Kessenbrock et al., 2010; Dudani et al., 2018; Wisdom et al., 2018). Recent progress in synthetic biology has constructed protease-responsive RNA polymerases (PRs) that can perform genetic circuits in live mammalian cells (Pu et al., 2015). Each protease-triggered proteolysis of PR releases an active RNA polymerase that enables the synthesis of multiple programmable RNA outputs, providing an effective strategy to amplify the signal of target protease activity. By designing the transcribed RNAs with a specific secondary structure exhibiting a high affinity toward specific fluorogenic ligands, we have developed a PR-based assay for the amplified detection of protease biomarkers with high sensitivity (Liu et al., 2020; Luo et al., 2020). This strategy not only addresses the limitation of lacking a signal amplification mechanism in the substrate peptide-based fluorescent methods (Roberts and Kelley, 2007; Cordovilla and Swager, 2012; Lee et al., 2020), but also circumvents the potential false positives derived from the undifferentiated recognition between target protease and its precursor by antibody in conventional immunoassays (Patel et al., 2011). Given the advantages of electrochemical testing techniques in simplicity, sensitivity, low cost, and miniaturization, it is worthwhile to explore the combination of PR and electrochemical interface for sensitive analysis of protease biomarkers.

The label-free electrochemical biosensor has gained increasing interest because of its simplicity and low cost in generating electrochemical signals (Zhang et al., 2010; Faria and Zucolotto, 2019; Shi et al., 2017; Liu et al., 2013). Herein, we presented a label-free electrochemical biosensor for the amplified detection of target protease biomarker by integrating electrochemical interface with proteolysis-triggered transcription. As shown in Scheme 1, each proteolysis of PR by target protease generates an active RNA polymerase, triggering the enzymatic synthesis of multiple programmable RNAs through in vitro transcription. The transcribed RNA comprises a guanine-rich sequence and the complementary sequence of the capture DNA probe immobilized on the gold electrode. After dropping the products of proteolysis-triggered transcription on the electrode, the transcribed RNAs can be captured and form G-quadruplex/hemin complexes in a buffer solution containing potassium ions and hemins. By measuring the electrochemical response of hemin on the electrode, label-free and amplified electrochemical detection of the target protease is achieved, providing a helpful tool for the clinical diagnosis of protease-related diseases. Unlike the previous works that use proteins or DNA as the output to generate electrochemical signals, this work converts target protease into RNA outputs, which represents a new strategy for the coupling of cell-free synthetic biology and electrochemical interface.

2. Experimental section

2.1. Reagents and materials

MMP-2, thrombin, Dimethyl sulfoxide (DMSO), 6-mercaptohexanol (MCH) and tris(2-carboxyethy) phosphine hydrochloride (TCEP) were provided by Sigma (St. Louis, MO, USA). Tris hydrochloride and 4-(2-hydroxyethyl) piperazine-1 ethanesulfonic acid sodium salt (HEPES) were purchased from Shanghai Sangon Biological Engineering Technology & Services Co., Ltd (Shanghai, China). MMP-3 was provided by PeproTech Inc. (Rocky Hill, NJ, USA). MMP-8 and MMP-9 were obtained from Sino Biological Inc. (Beijing, China). Furin was provided by New England Biolabs (Beijing, China). T7 RNAP, DNase I and rNTPs (rATP, rUTP, rCTP and rGTP) were obtained from Thermo Scientific (Thermo Scientific, Waltham, MA). ARP 100 was provided by Santa Cruz Biotechnologies (USA). Cell culture medium (DMEM and RPMI-1640), trypsin and fetal bovine serum (FBS) were obtained from Invitrogen (Gibco, USA). Hemin was purchased from Aladdin Reagents (Shanghai, China). The hemin was dissolved in DMSO to stock solutions with 10 mM and stored at −20 °C. Besides, the HPLC-purified oligonucleotide sequences (Supplemental Table S1) were synthesized and purified by Sangon Biotech Co., Ltd. (Shanghai, China). Stock solutions (100 μM) of the oligonucleotides were prepared with DEPC-treated water and stored at −20 °C before use. All chemicals were of analytical grade and all solutions were prepared with ultrapure water (specific resistance of 18.25 MΩ cm).

2.2. Enzymatic hydrolysis of PR_{MMP-2}

The construction, expression and purification of PR_{MMP-2} protein were according to the previously reported literature (Liu et al., 2020). For the detection of target MMP-2, different concentrations of MMP-2 were added into 10 μL of reaction solution (40 mM Tris, 9.0 mM $MgCl_2$, 10 mM NaCl, 100 mM KCl, 2.0 mM spermidine, 10 mM DTT and pH 7.5) containing 1.0 μM PR_{MMP-2}, 5.0 mM rNTPs and 1.0 μM DNA template. All components were mixed and incubated at 37 °C for 2 h.

2.3. Gel electrophoresis studies

SDS-PAGE was used to analyze the degradation of PR_{MMP-2} by the target MMP-2. Specifically, 10 μL of the proteolysis reaction solution was loaded and analyzed by 10% denatured polyacrylamide gels at 110 V for 90 min. We employed native PAGE to analyze the hybridization between transcribed RNA and DNA, 10 μL solution was loaded and analyzed by 12% polyacrylamide gels (39:1 acrylamide/bisacrylamide) at 110 V for 2.5 h. Then the gel was stained by GelRed (diluted 1:10000) for 30 min. Then, the gels were scanned under UV light using a

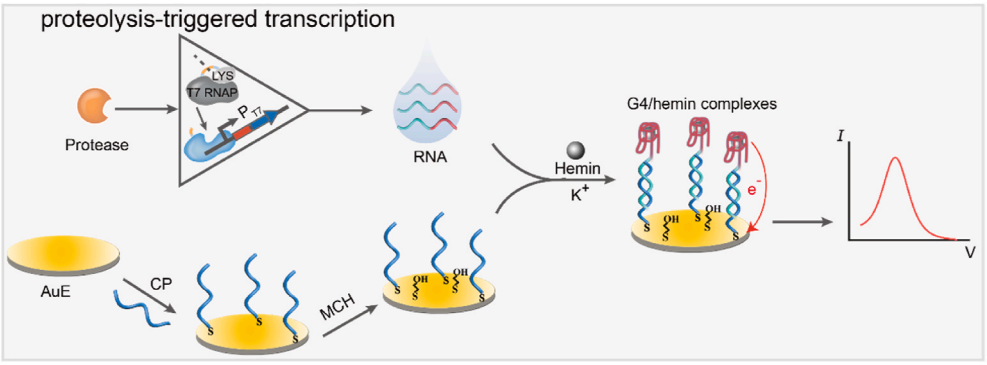

Scheme 1. Schematic illustration of PR-based electrochemical biosensor for label-free and amplified detection of target protease. LYS-T7 RNAP: T7 lysozyme and T7 RNA polymerase fusion protein; PT7: T7 promoter; AuE; gold electrode; CP: capture DNA probe; MCH: mercaptohexanol; G4: G-quadruplex.

ChemiDoc™ MP system (Bio-Rad, USA).

2.4. Electrode preparation and sensor fabrication

The electrodes were prepared using a well-established procedure described by Kang et al. with minor alterations (Kang et al., 2009). In brief, gold electrodes (AuEs, 3 mm in diameter) were first cleaned both mechanically (by polishing with 0.3 and 0.05 μm alumina oxide slurries successively) and electrochemically (through successive scans between −0.3 and 1.5 V in a fresh 0.5 M H_2SO_4 solution). After being rinsed thoroughly and dried with nitrogen, the AuEs should be immediately used for CP immobilization.

The above AuEs were then incubated with 0.5 μM pretreated CP in immobilization buffer solution (10 mM Tris-HCl, 1.0 mM EDTA, 1.0 mM TCEP, 1.0 mM $MgCl_2$ and 0.1 M NaCl, pH 7.4) for 12 h at 25 °C. Next, to remove the nonspecific adsorption, the resulting CP-assembled AuEs were immersed 3 mM MCH in deionized water for 1 h to obtain the MCH/CP/AuE. Followed by being rinsed and dried, 10 μL of the transcription reaction mixture was dropped on the MCH/CP/AuE and incubated for 2 h at 37 °C. Therefore, the CP probes capture the transcribed RNA to form CP/RNA duplex structure through hybridizations on the AuE surface. After that, the resulting AuEs were incubated with 0.2 mM freshly prepared hemin in 20 mM HEPES buffer (50 mM KCl, 200 mM NaCl, 1% DMSO, pH 8.0) for 30 min at 25 °C to allow the assembly of hemin with G-quadruplex. After incubating the cell-free reactants on the electrode and the hemin and K^+ solutions, the electrode was carefully rinsed with 20 mM HEPES buffer (50 mM KCl, 200 mM NaCl and pH 8.0) before the electrochemical detections.

2.5. Electrochemical measurements

All electrochemical measurements were conducted on a CHI 660 A workstation (CH Instruments, Shanghai, China). The platinum wire, saturated calomel electrode (SCE) and AuE were used as the auxiliary electrode, reference electrode and working electrode in all the experiments, respectively. The cyclic voltammetry (CV) was carried out in 0.1 M KCl solution containing 5.0 mM $Fe(CN)_6^{3-/4-}$ by scanning the potential from −0.1 to 0.6 V under a scan rate of 50 mV s^{-1}. The electrochemical impedance spectroscopy (EIS) was performed in 0.1 M KCl aqueous solution with 5.0 mM $[Fe(CN)_6]^{3-/4-}$ as the probe in the frequency range from 0.1 Hz to 100 kHz with 5.0 mV as the amplitude at a potential of 0.22 V (vs. SCE). The differential pulse voltammetry (DPV) measurements were performed with the potential window from −0.15 to −0.5 V with pulse amplitude of 50 mV, pulse width of 25 ms and sample width of 16.7 ms in 20 mM HEPES buffer (50 mM KCl, 200 mM NaCl and pH 8.0). The buffer solution was degassed with high purity nitrogen for 30 min to avoid the interference from the reduction of oxygen.

2.6. Analysis of MMP-2 activity in biological samples

For the detection of MMP-2 expression levels in different cell cultures by the proposed biosensor, two cell lines (HepG2 and LO2) were chosen as the model. The cells were cultured in 35 mm dishes with DMEM or RPMI-1640 containing 10% FBS under a humidified atmosphere of 5% CO_2 at 37 °C. When 80% confluence was reached, HepG2 and LO2 cells were washed three times with PBS and starved for 36 h in DMEM or RPMI-1640 without FBS. After that, the secreted MMP-2 was obtained by centrifugation (12000 rpm, 10 min) to remove cells and cell debris from the conditioned medium. Finally, the extracted total proteins were enriched 2.5 times by freeze-drying and then resuspended in water stored at −20 °C.

For the detection of MMP-2 expression level in osteosarcoma and paracancerous tissue samples, tissue samples of 6 patients (1 woman and 5 men; mean age 28 years, range 16–48 years) were obtained from the Second Xiangya Hospital, Central South University (China, Hunan). The sampling of clinical tissues was approved by the local institutional review committee and agreed by all subjects. Tissue sample processing and crude protein extraction were carried out according to previous reports (Liu et al., 2020). Finally, the total expression of MMP-2 in different cells (1 mg/mL total proteins) and osteosarcoma tissues (10 mg/mL total proteins) were directly measured with this sensor.

3. Results and discussion

3.1. Integration of in vitro transcription and electrochemical interface

In this work, the implementation of the PR-based electrochemical protease sensor primarily relies on the efficient integration of in vitro transcription and electrochemical interface. To this end, we sought to integrate T7 RNA polymerase-catalyzed in vitro transcription with capture DNA probe (CP)-modified electrochemical interface (Fig. 1A). The RNA generated by in vitro transcription was designed to contain the complementary sequence of CP. The hybridization between transcribed RNA and CP was confirmed by native polyacrylamide gel electrophoresis (Fig. 1B). The CP with a thiol modification at 3′-terminus could self-assemble on the surface of a gold electrode (AuE) through the formation of Au–S bonds, and then the surface was blocked with MCH for the preparation of an electrochemical interface. After that, the transcription products were dropped on the AuE for the formation of RNA/CP duplexes. Next, we employed cyclic voltammetry (CV) to characterize each reaction step of the electrochemical interface. As shown in Fig. 1C, a pair of well-defined redox peaks could be noticed, implying excellent capability of electron transport of bare AuE (curve a). After the stepwise assembly of CP and MCH on the AuE, the redox current remarkably decreased (curve b and c), because of the electrostatic repulsion between negative charges of DNA backbones and $Fe(CN)_6^{3-/4-}$ as well as the blocking effect of MCH. Then, the capture of transcribed RNA led to a further reduction and peak-to-peak separation in the CV signal (curve d, Table S2) due to the introduction of more negative charges onto the surface of AuE. Additionally, electrochemical impedance spectroscopy (EIS) was further employed to investigate the stepwise fabrication process of the electrochemical interface (Fig. 1D). As shown in Fig. 4D The charge transfer resistance (R_{ct}) of AuE increased from 116.6 Ω to 1478 Ω after the modification of CP (curves a and b). After blocking by MCH, the value increased to 2383 Ω (curve c). Moreover, it further increased to 3481 Ω (curve d) upon the incubation with transcribed RNA. Based on the CV and EIS results, we could conclude that efficient integration of in vitro transcription and electrochemical interface has been achieved by rational design of the transcribed RNA.

3.2. Construction of the PR-based electrochemical protease sensor

Having realized the integration of in vitro transcription and electrochemical interface, we next sought to investigate the feasibility of the PR-based electrochemical protease sensor by employing MMP-2 as a model case. MMP-2 is an essential protease in the process of tumor growth, invasion and metastasis because it primarily hydrolyzes collagen VI (Zeng et al., 1999; Kessenbrock et al., 2010). Therefore, the development of simple, sensitive and low-cost approaches for the detection of MMP-2 is of great significance for the clinical diagnosis of cancer (Li et al., 2014; Kou et al., 2017; Li et al., 2020). Here, our previously constructed $PR_{MMP\text{-}2}$ with responsivity toward MMP-2 was adopted to develop the PR-based electrochemical protease sensor by integrating with the electrochemical interface (Fig. 2A). The $PR_{MMP\text{-}2}$ was constructed by tethering an inhibitory protein to the N-terminus of T7 RNA polymerase through a peptide linker containing the substrate sequence recognized by MMP-2 (Liu et al., 2020). In the $PR_{MMP\text{-}2}$, the catalytical activity of T7 RNA polymerase is inhibited. While the specific cleavage of the linker by MMP-2 results in the release of an active T7 RNA polymerase. To investigate the cleavage of $PR_{MMP\text{-}2}$ toward MMP-2, we analyzed the proteolysis product of $PR_{MMP\text{-}2}$ by SDS-PAGE and MALDI-TOF MS, respectively. The appearance of the band

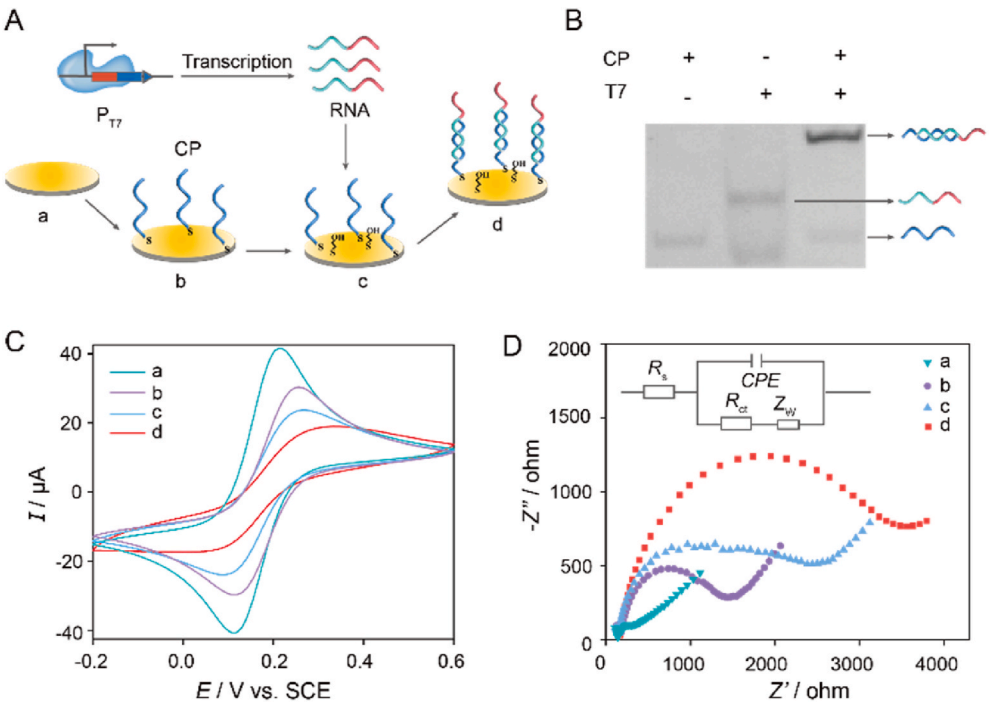

Fig. 1. (A) Schematic illustration of the integration of T7 RNAP-mediated transcription and electrochemical interface. (B) Analysis of the hybridization between transcribed RNA and CP by native polyacrylamide gel electrophoresis (12%). The transcription products were pretreated with DNase I (5.0 U) to digest the template DNA. (C) Typical CV and (D) EIS responses of different modified electrodes: bare AuE (a), AuE/CP (b), AuE/CP/MCH (c), and AuE/CP/MCH/RNA (d) in 0.1 M KCl solution containing 5.0 mM $[Fe(CN)_6]^{3-/4-}$. T7 RNAP, 4.0 U; DNA template, 1.0 μM; and CP, 0.5 μM. R_S and R_{ct} are the solution resistance and charge transfer resistances, respectively. Z_W is the Warburg impedance resulting from the diffusion of ions from the bulk of the electrolyte to interface. *CPE* is the constant phase element of the electrode surface/solution interface.

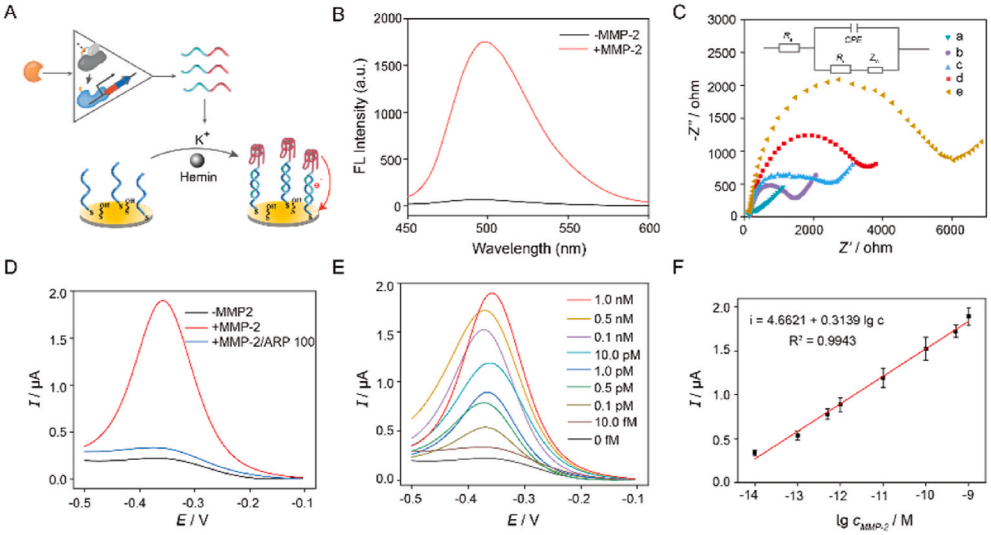

Fig. 2. (A) Schematic presentation of the construction of PR-based electrochemical protease biosensor. (B) Fluorescence emission spectra of the transcription products lit up by Thioflavine-T in the absence and presence of MMP-2 (1.0 nM). (C) EIS responses of the electrode with different modifications: bare AuE (a), AuE/CP (b), AuE/CP/MCH (c), AuE/CP/MCH/RNA (d), AuE/IP/MCH/RNA/hemin (e). CP, 0.5 μM; hemin, 0.2 mM; and MMP-2, 1.0 nM. (D) Typical DPV responses of the blank, MMP-2 and MMP-2 pretreated with ARP100. MMP-2, 1.0 nM; and ARP 100, 100 nM. (E) Typical DPV responses of MMP-2 different concentrations. (F) Calibration curves of the biosensor responding to different concentrations of MMP-2. Data represent means ± SD; n = 3.

corresponding to T7 RNA polymerase in gel image (Fig. S1) and the emergence of the peak of T7 RNA polymerase in MS spectra (Fig. S2) collectively elucidated the effective proteolysis of PR_{MMP-2}. Then, whether the RNAs generated by MMP-2-triggered transcription can form a G-quadruplex structure was studied using a specific fluorogenic ligand. An intensive fluorescence signal was observed in the presence of MMP-2 (Fig. 2B), suggesting the formation of G-quadruplex structure as expected. Moreover, the formation of G-quadruplex/hemin complexes was demonstrated by the redshift of the Soret band of hemin from 397 nm to 404 nm (Fig. S3) and the color reaction catalyzed by the peroxidase-like activity (Fig. S4).

Next, the RNAs generated by MMP-2-triggered transcription were captured on the surface of CP-modified AuE, followed by the incubation with hemin in the presence of potassium ions. The formation of G-quadruplex/hemin complexes on AuE was preliminarily confirmed by the apparent increase in electrochemical impedance (Fig. 3C). Next, the electrochemical response was determined by differential pulse voltammetry (DPV). As shown in Fig. 4D, the appearance of a DPV peak current at around −0.35 V is corresponding to the reversible Fe(III)/Fe(II) redox of hemin, directly demonstrating the formation of G-quadruplex/hemin complexes on AuE (Zhu et al., 2008; Funabashi, 2016). Moreover, the sharp decrease in DPV peak current (declined 85.1%) when MMP-2 was pretreated with ARP 100 (a specific inhibitor of MMP-2), indicating that the electrochemical signal was derived from the G-quadruplex/hemin complexes generated by MMP-2-triggered transcription. Then, the effects of several important reaction conditions on the analytical performance, including the amount of CP, hybridization time and the concentration of hemin, were investigated. The corresponding optimized values were determined to be 0.5 μM, 120 min and 0.2 mM, respectively (Figs. S5–S7).

Under the optimized conditions, the electrochemical responses of MMP-2 at different concentrations by the PR-based electrochemical

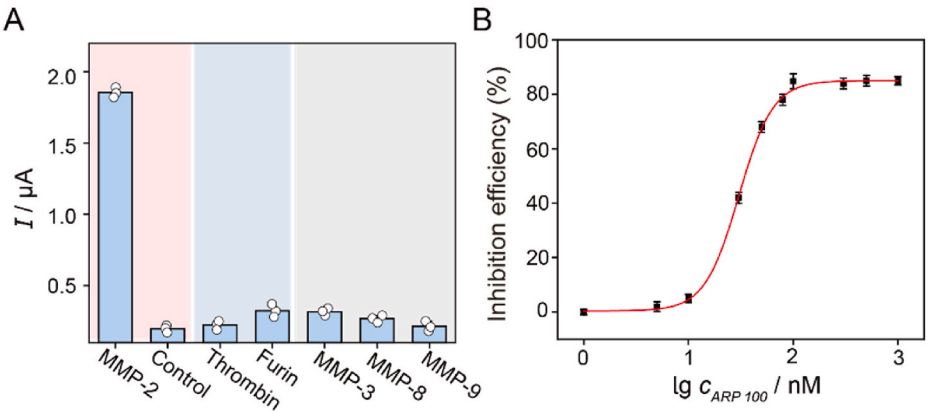

Fig. 3. (A) DPV peak current signals of PR-based electrochemical biosensor in response to MMP-2 (1.0 nM) and other proteases (5.0 nM), respectively. (B) Dose-dependent inhibition curve of ARP 100 on the activity of MMP-2 (1.0 nM). Data represent means ± SD; n = 3.

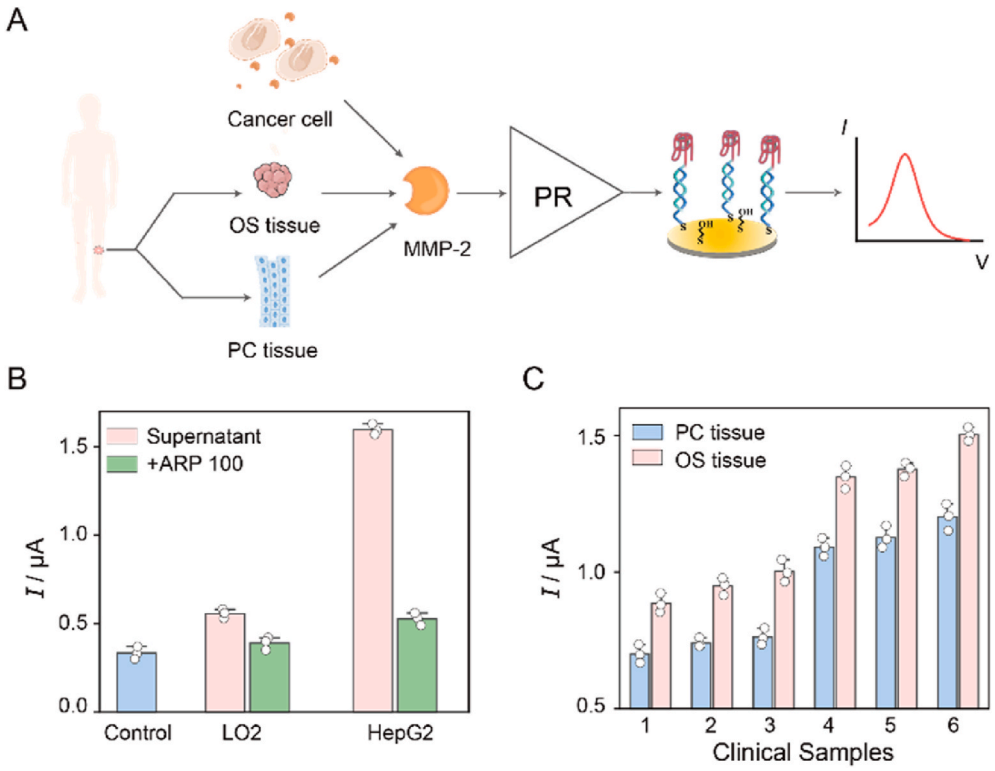

Fig. 4. (A) Schematic illustration for the detection of cancer-associated MMP-2 in cell cultures and human tissue samples by PR-based electrochemical biosensor. (B) Typical DPV signals of the cell culture supernatants from different cell lines without and with the pretreatment of ARP 100 (100 nM). (C) Typical DPV signals of MMP-2 expression level detection in OS and PC tissue samples from 6 OS patients. Data represent means ± SD; n = 3.

biosensor were investigated. As the concentration of MMP-2 increased from 10 fM to 1.0 nM, the DPV peak current gradually increased from 0.25 to 1.88 μA (Fig. 2E). There was a linear relationship between DPV peak current and the logarithm of MMP-2 concentration in the range of 10 fM-1.0 nM, with the linear regression equation of i = 4.6621 + 0.3139 lg c (R^2 = 0.9943). According to the 3σ rule, the limit of detection was determined to be 7.1 fM, which was much lower than that in many previously reported methods (Table S3). Moreover, six repetitive measurements of target DNA at 1.0 pM yielded a relative standard deviation of 3.9% (Fig. S8), indicating the good reproducibility of the proposed biosensor. Taken together, by integrating proteolysis-triggered transcription with the electrochemical interface, we have constructed a PR-based electrochemical biosensor that enables the detection of target protease with femtomolar sensitivity.

3.3. Specificity and potential in inhibitor screening

In addition to high sensitivity, reasonable specificity is also an important parameter in the clinical diagnosis of protease biomarkers. Since many proteolysis reactions might occur in the complicated cellular microenvironment, the potential influences from other cellular proteases need to be evaluated. To investigate the specificity of the PR-base electrochemical biosensor on the detection of MMP-2, we chose five kinds of proteases, including thrombin, furin and other types of MMPs (e.g., MMP-3, MMP-8 and MMP-9), as the potential interferents. As displayed in Fig. 3A and Fig. S9, MMP-2 induced a remarkable DPV signal, while the other proteases at a higher concentration (5 times) could only cause a slight response, which indicates the high specificity of the PR-based electrochemical biosensor for the detection of MMP-2.

Next, the applicability of the proposed electrochemical biosensor in the evaluation of the inhibitory effect on MMP-2 activity by small molecules was studied. A specific inhibitor of MMP-2 (ARP 100) was selected as the model, and it has been validated to have no influence on theT7 RNA polymerase-mediated in vitro transcription. When the concentration of ARP 100 increased from 1.0 to 1000 nM, the DPV peak current declined gradually (Fig. S10). A dose-dependent inhibition curve was obtained with an IC50 value of 44.7 nM (Fig. 3B), implying the potential of this electrochemical biosensor in screening the inhibitors of target protease.

3.4. Evaluation of MMP-2 levels in biological samples

Encouraged by the high sensitivity and specificity of this PR-based electrochemical biosensor, we further evaluated its practical unity on the detection of MMP-2 activity in complex biological samples (Fig. 4A). Previous reports demonstrated that active MMP-2 is upregulated in human cancer cells and various human cancer tissues (Kenny and Lengyel, 2009; Roy et al., 2009). Here, human hepatoma carcinoma cells (HepG2) and human hepatocyte cells (LO2) were chosen as the models. The culture supernatants of these cells were isolated for the subsequent tests. The testing results were shown in Fig. 4B, and only a slight DPV signal was observed in the LO2 cell group. On the contrary, the group of HepG2 cells induced a drastic response in DPV peak signal that is 2.9 times as high as that of LO2 cell group, which might be associated with the upregulated expression levels of MMP-2 tumor cells. When the cells were pretreated with ARP 100, the DPV signals decreased to the level of the blank group, indicating that the proteolysis reactions catalyzed by MMP-2 specifically generated the signals.

Next, we sought to employ this electrochemical biosensor to analyze MMP-2 activity in clinical samples. Previous studies revealed that MMP-2 involves in the malignant and metastatic of Osteosarcoma (OS). We analyzed the MMP-2 activity in OS and paracancerous (PC) tissues from 6 patients by the PR-based electrochemical protease biosensor. Crude proteins extracted from PC and OS tissues were tested, and the results were shown in Fig. 4C. Elevated DPV signals of MMP-2 activity could be detected in all OS tissues compared with the PC tissues. Moreover, the pretreatment with ARP 100 induced a sharp decrease in the DPV signals in both PC and OS groups, suggesting a high level of MMP-2 activity in these tissues (Thomas et al., 2000; Kun-Peng et al., 2017). Together, these results indicate the potential of this PR-based electrochemical biosensor in the analysis of target protease biomarkers in clinical samples.

4. Conclusions

In summary, we proposed an electrochemical biosensor that allows for the label-free and amplified detection of target protease biomarker. This biosensor was constructed by the rational integration of proteolysis-triggered transcription and the electrochemical interface. Owing to efficient integration of in vitro transcription-mediated signal amplification and the superior sensitivity of the electrochemical testing technique, this PR-based electrochemical achieved the specific detection of the MMP-2 biomarker with femtomolar sensitivity. Moreover, the feasibility of this biosensor was also demonstrated by the sensitive assessment of MMP-2 levels in biological samples, suggesting its potential applications in basic biomedical research and clinical disease diagnosis. PRs with different target responsivities can be facilely constructed by tuning the liner sequence (Liu et al., 2020); and thus PR-based electrochemical biosensors for other protease biomarkers can be fabricated by simply replacing the PR module. Moreover, by employing orthogonal PRs (Pu et al., 2015) and designing orthogonal outputs of transcribed RNAs, simultaneous and multiplexed electrochemical analysis of several kinds of protease biomarkers is expected realize by using electrode arrays. Therefore, this work has offered a feasible paradigm to integrate cell-free synthetic biology strategy with the electrochemical interface, which will boost the research on their advanced integrations to exploit more potent and applicable applications for clinical diagnosis.

CRediT authorship contribution statement

Kai Shi: designed the study, performed experiments, Formal analysis, and drafted the manuscript. **Lei Cao:** Formal analysis. **Fang Liu:** constructed the plasmid. **Shiyi Xie:** Formal analysis. **Shuo Wang:** Formal analysis. **Yan Huang:** Supervision. **Chunyang Lei:** Writing – original draft, Conceptualization. **Zhou Nie:** Supervision.

Declaration of competing interest

The authors declare that they have no known competing financial interests or personal relationships that could have appeared to influence the work reported in this paper.

Acknowledgements

This work was supported by the National Natural Science Foundation of China (21974038, 22074034 and 21725503), the Natural Science Foundation of Hunan Province (2020JJ5037) and the Fundamental Research Funds for the Central Universities.

Appendix A. Supplementary data

Supplementary data to this article can be found online at https://doi.org/10.1016/j.bios.2021.113372.

References

Ausländer, S., Ausländer, D., Fussenegger, M., 2017. Angew. Chem. 56, 6396–6419.
Bordusa, F., 2002. Chem. Rev. 102, 4817–4867.
Bories, D., Raynal, M.-C., Solomon, D.H., Darzynkiewicz, Z., Carye, Y.E., 1989. Cell 59, 959–968.
Carlson, E.D., Gan, R., Hodgman, C.E., Jewett, M.C., 2012. Biotechnol. Adv. 30, 1185–1194.
Cordovilla, C., Swager, T.M., 2012. J. Am. Chem. Soc. 134, 6932–6935.
Courbet, A., Endy, D., Renard, E., Molina, F., Bonnet, J., 2015. Sci. Transl. Med. 7, 289ra83.
Dai, Y.F., Xu, W., Somoza, R.A., Welter, J.F., Caplan, A.I., Liu, C.C., 2020. Angew. Chem. Int. Ed. 59, 20541–20545.
Demeyer, A., Staal, J., Beyaert, R., 2016. Trends Mol. Med. 22, 135–150.
Dudani, J.S., Ibrahim, M., Kirkpatrick, J., Warren, A.D., Bhatia, S.N., 2018. Proc. Natl. Acad. Sci. U.S.A. 115, 8954–8959.
Faria, H.A.M., Zucolotto, V., 2019. Biosens. Bioelectron. 131, 149–155.
Funabashi, H., 2016. Electrochemistry 84, 290–295.
Haass, C., Strooper, B.D., 1999. Science 286, 916–919.
Hua, X.Y., Yang, E.F., Yang, W.T., Yuan, R., Xu, W.J., 2019. Chem. Commun. 55, 12463–12466.
Jung, J.K., Alam, K.K., Verosloff, M.S., Capdevila, D.A., Desmau, M., Clauer, P.R., Lee, J. W., Nguyen, P.Q., Pastén, P.A., Matiasek, S.J., Gaillard, J.F., Giedroc, D.P., Collins, J., Lucks, J.B., 2020. Nat. Biotechnol. 6, 1–9.
Kang, T., Wei, Y., Honaker, Y., Yamaguchi, H., Appella, E., Hung, M.-C., Piwnica-Worms, H., 2008. Canc. Cell 13, 36–47.
Kang, D., Zuo, X.L., Yang, R.Q., Xia, F., Plaxco, K.W., White, R.J., 2009. Anal. Chem. 81, 9109–9113.
Keasling, J.D., 2012. Metab. Eng. 14, 189–195.
Kenny, H.A., Lengyel, E., 2009. Cell Cycle 8, 683–688.
Kessenbrock, K., Plaks, V., Werb, Z., 2010. Cell 141, 52–67.
Kopniczky, M.B., Canavan, C., McClymont, D.W., Crone, M.A., Suckling, L., Goetzmann, B., Siciliano, V., MacDonald, J.T., Jensen, K., Freemont, P.S., 2020. ACS Synth. Biol. 9, 144–156.
Kotula, J.W., Kerns, S.J., Shaket, L.A., Siraj, L., Collins, J., Way, J.C., Silver, P.A., 2014. Proc. Natl. Acad. Sci. U.S.A. 111, 4838–4843.
Kou, B.-B., Chai, Y.-Q., Yuan, Y.-L., Yuan, R., 2017. Anal. Chem. 89, 9383–9387.
Kun-Peng, Z., Chun-Lin, Zhang, Xiao-Long, M., 2017. Int. J. Biol. Sci. 13, 1180–1191.
Lee, H., Kim, S.-j., Shin, H., Kim, Y.-P., 2020. ACS Sens. 5, 655–664.
Li, X., Deng, D.W., Xue, J.P., Qu, L.Z., Achilefu, S., Gu, Y.Q., 2014. Biosens. Bioelectron. 61, 512–518.
Li, Y.Y., Liu, W., Xu, Q.F., Hu, J., Zhang, C.-Y., 2020. Biosens. Bioelectron. 169, 112467.
Liu, S.F., Wang, C.F., Zhang, C.X., Wang, Y., Tang, B., 2013. Anal. Chem. 85, 2282–2288.
Liu, F., Yang, M., Song, W.L., Luo, X.Y., Tang, R., Duan, Z.X., Kang, W.Y., Xie, S.Y., Liu, Q.Q., Lei, C.Y., Huang, Y., Nie, Z., Yao, S.Z., 2020. Chem. Sci. 11, 2993–2998.
Lo, E.H., Wang, X.Y., Cuzner, M.L., 2002. J. Neurosci. Res. 69, 1–9.
Luo, X.Y., Zhao, J.L., Xie, Xuan, Liu, Fang, Zeng, Pan, Lei, C.Y., Nie, Z., 2020. Anal. Chem. 92, 16314–16321.

Mimee, M., Nadeau, P., Hayward, A., Carim, S., Flanagan, S., Jerger, L., Collins, J., McDonnell, S., Swartwout, R., Citorik, R.J., Bulović, V., Langer, R., Traverso, G., Chandrakasan, A.P., Lu, T.K., 2018. Science 360, 915–918.
Mousavi, P.S., Smith, S.J., Chen, J.B., Karlikow, M., Tinafar, A., Robinson, C., Liu, W.H., Ma, D., Green, A.A., Kelley, S.O., Pardee, K., 2020. Nat. Chem. 12, 48–55.
Patel, S., Sumitra, G., Koner, B.C., Saxena, A., 2011. Clin. Biochem. 44, 869–872.
Pu, J.Y., Chronis, I., Ahn, D., Dickinson, B.C., 2015. J. Am. Chem. Soc. 137, 15996–15999.
Riglar, D.T., Giessen, T.W., Baym, M., Kerns, S.J., Niederhuber, M.J., Bronson, R.T., Kotula, J.W., Gerber, G.K., Way, J.C., Silver, P.A., 2017. Nat. Biotechnol. 35, 653–658.
Roberts, M.A., Kelley, S.O., 2007. J. Am. Chem. Soc. 129, 11356–11357.
Roy, R., Yang, J., Moses, M.A., 2009. J. Clin. Oncol. 27, 5287–5297.
Saltepe, B., Bozkurt, E.U., Güngen, M.A., Cicek, A.E., Şeker, U.Ö.Ş., 2021. Biosens. Bioelectron. 178, 113028.
Shi, K., Dou, B.T., Yang, J.M., Yuan, R., Xiang, Y., 2017. Biosens. Bioelectron. 87, 495–500.
Silver, A.D., Akova, U., Alam, K.K., Jewett, M.C., Lucks, J.B., 2020. ACS Synth. Biol. 9, 671–677.
Thomas, P., Khokha, R., Shepherd, F.A., Feld, R., Tsao, M.-S., 2000. J. Pathol. 190, 150–156.
Turk, B., 2006. Nat. Rev. Drug Discov. 5, 785–799.
Wan, X., Volpetti, F., Petrova, E., French, C., Maerkl, S.J., Wang, B., 2019. Nat. Chem. Biol. 15, 540–548.
Wang, X.Z., Dong, S.S., Gai, P.P., Duan, R., Li, F., 2016. Biosens. Bioelectron. 82, 49–54.
Watstein, D.M., Styczynski, M.P., 2018. ACS Synth. Biol. 7, 267–275.
Wisdom, K.M., Adebowale, K., Chang, J., Lee, J.Y., Nam, S., Desai, R., Rossen, N.S., Rafat, M., West, R.B., Hodgson, L., Chaudhuri, O., 2018. Nat. Commun. 9, 4144.
Zeng, Z.S., Cohen, A.M., Guillem, J.G., 1999. Carcinogenesis 20, 749–755.
Zhang, K., Zhu, X.L., Wang, J., Xu, L.L., Li, G.X., 2010. Anal. Chem. 82, 3207–3211.
Zhu, X.L., Zhang, W.J., Han, X., Huang, J.Y., Li, G.X., 2008. Electrochim. Acta 53, 4407–4413.